Expanding the spectrum of early neuroradiological findings in Beta Propeller Protein-Associated Neurodegeneration (BPAN)

Apostolos Papandreou[1, 2], Audrey KS Soo[1, 2], Robert Spaull[1, 2], Kshitij Mankad[3], Manju A Kurian[1, 2]*, Sniya Sudhakar[3]*

Affiliations

1. Molecular Neurosciences, Developmental Neurosciences Programme, Zayed Centre for Research into Rare Disease in Children, University College London Great Ormond Street Institute of Child Health, London, UK

2. Department of Neurology, Great Ormond Street Hospital for Children NHS Foundation Trust, London, UK

3. Department of Neuroradiology, Great Ormond Street Hospital for Children NHS Foundation Trust, London, UK

* These authors contributed equally

Correspondence:

Dr Apostolos Papandreou MBBS MRCPCH PhD

NIHR GOS BRC Catalyst Fellow

University College London GOS Institute of Child Health;

Honorary Consultant Paediatric Neurologist

Evelina London Children's Hospital

London, UK

Email: Apostolos.papandreou@ucl.ac.uk

Abstract

Background and Purpose

Beta Propeller Protein-Associated Neurodegeneration (BPAN) is the most common Neurodegeneration with Brain Iron Accumulation disorder. Typical radiological findings are T2 hypo-intensity in the Substantia Nigra (SN) and Globus Pallidus (GP), as well as a T1 halo-like SN hyper-intense signal surrounding a hypo-intense central area. However, these findings are often subtle or absent on initial scans, risking diagnostic delay. In this study, we sought to investigate radiological findings that could aid early diagnosis of BPAN.

Materials and Methods

A retrospective cohort study was performed in a national referral center, including all pediatric patients with confirmed pathogenic *WDR45* mutations and consistent clinical semiology. Magnetic resonance imaging findings were independently reported by two pediatric neuroradiologists.

Results

Fifteen patients were included in the study and 27 scans were available for review. Initial neuroimaging study was undertaken at a mean age of 3.2 years. Iron deposition was uncommon in patients under 4 years of age. Neuroradiological features from very early on included dentate, globus pallidus and substantia nigra swelling, as well as thin corpus callosum and small pontine volume. Optic nerve thinning was also present in all patients.

Conclusion

Our study highlights the key early MRI features of BPAN. Iron deposition in the globus pallidus and substantia nigra is not common under 4 years of age; clinicians should not be deterred from suspecting BPAN in presence of the findings described in this study and the appropriate clinical context.

Introduction

Beta Propeller Protein-Associated Neurodegeneration (BPAN) is emerging as the most common Neurodegeneration with Brain Iron Accumulation (NBIA) disorder[1]. It is caused by mutations in *WDR45*, an X-linked gene with a role in early autophagy[2, 3]. Clinically, it typically manifests in infancy with neurodevelopmental delay, epilepsy, autistic-like features, other behavioral issues, stereotypies, and sleep disturbance. Following a relatively stable course in childhood, BPAN progresses in adolescence or early adulthood with motor regression, dementia, and parkinsonian features[1-3]. A core radiological and neuropathological hallmark is brain iron accumulation, most prominently in the substantia nigra (SN) but also in the globus pallidus (GP)[1, 3, 4]. The classically reported magnetic resonance imaging (MRI) findings are SN and GP hypointensity on T2-weighted sequences, as well as a 'halo-like' SN hyperintensity with a central hypointense band on T1-weighted images[3, 5, 6]. Case reports and small cohort studies have described additional BPAN-related findings such as SN swelling, delayed myelination, corpus callosum (CC) thinning, deep cerebellar nuclei T2 hyperintensities and cerebellar atrophy[5, 7]. However, these features are often either absent on initial scans or not specific enough to aid diagnosis.

BPAN is a rare disease, with an estimated prevalence of 1 in 2-3 million individuals[1]. Due to this rarity, and non-specific clinical presentation at disease onset, the diagnosis is frequently not suspected and only made when non-selective genetic testing (gene panel, exome or genome sequencing) reveals a *WDR45* pathogenic variant. Prompt establishment of a BPAN diagnosis is crucial for accurate prognosis, genetic counselling, and appropriate multidisciplinary management[1]. Should disease-specific therapies emerge in the future, as has recently happened for many neurometabolic conditions[8], the need for an accurate diagnosis will become even more pertinent. However, there are currently no BPAN-specific biochemical or early radiological markers[1, 9], and genetic variants of unknown significance can be very difficult to interpret.

In this study, we evaluated a cohort of children with BPAN presenting to a single pediatric center and identified several neuroradiological keys that may facilitate early diagnosis of this disease.

Methods

The study was approved by the Great Ormond Street Hospital Research and Development Audit Department (reference: 3261). All data was anonymized by the lead care teams at the point of collection, so the study did not otherwise require ethical approval.

We undertook a single center cohort study on patients with an established diagnosis of BPAN attending a UK pediatric neurogenetic clinic. Inclusion criteria included disease of childhood onset (0-18 years of life), the presence of a pathogenic *WDR45* genetic variant, and clinical semiology consistent with BPAN. Characterization of the clinical phenotype was undertaken by direct clinical examination and case note review.

Brain MRIs had either been performed at Great Ormond Street Hospital or at the referring local hospital and subsequently transferred for neuroradiology review. Different machine models and specifications were used for image acquisition. Brain MRIs were individually reviewed for quality, and read by 2 of the authors (K.M and S.V.), with subsequent discussion for disparate opinion in order to reach consensus agreement. Specifically, T2-weighted signal intensity and swelling of dentate nuclei, GP and SN; T1-weighted signal of SN; Susceptibility-Weighted Imaging (SWI) signal changes where available; morphology and size of brainstem; and the rest of the brain parenchyma were assessed. Optic nerves were also assessed and measured in the pre-chiasmatic segments on T2 and T1-weighted axial sequences; for this, 3mm to 5mm slice thickness images were used, depending on availability, while other planes were also used for correct localization. Cerebral and cerebellar atrophy was subjectively graded as mild, moderate, and severe. Cerebellar atrophy was further qualified as vermian (including gradient, if any), hemispheric or both. Volumetric analysis was not performed due

to insufficient numbers of cases with volume data. Data were analyzed with descriptive statistics.

Results

Patient Cohort

16 paediatric patients were identified. Some cases have previously been reported[10] (**Table 1**). Neuroimaging was available for 15/16 patients. Mean and median ages at last clinical review for patients having undergone neuroimaging were 10.5 and 9.95 years, respectively (age range 3.9 to 22 years). Mean and median ages at scanning were 4.3 and 3 years, respectively. As expected, most (13/15) patients were female. Common clinical manifestations included early infantile-onset developmental delay (15/15), epilepsy (13/15), sleep disturbances (5/15), stereotypies (5/15), and febrile seizures (2/15). Non-stereotypy movement disorders were uncommon, as expected in this age group[1] with parkinsonian features (1/15), tremor (1/15), dystonia (2/15) and spasticity rarely described.

A single MRI brain scan was available for 5/15 cases, whereas 8/15 had 2 scans and 2/15 had 3 scans in total. Age at scanning ranged from 0.8 to 14 years (mean and median 3.9 and 3 years, respectively). The first MRI was undertaken at a mean age of 3.2 years, whereas the second and third at mean ages of 5.6 and 5.8 years, respectively. Time between follow up scans ranged from 1.1 to 9.1 years.

Radiological Findings (Figures 1-2, Tables 1 and 2)

27 MRI scans were available from 15 children.

Firstly, dentate nucleus abnormalities with T2-weighted hyperintensity, and swelling or prominence, were seen in 26/27 scans, except in patient B9 who had only a single scan at 14 years of age.

Regarding the GP, swelling was seen in 26/27 scans, except in patient B14's second scan at 3 years of age. GP signal T2-hyperintensity was observed in 11/27 scans, but mostly in the

younger age groups (the oldest scan at 5 years 5 months of age). In children over 5 years old, GP was either isointense or hypointense compared to the striatum and red nucleus. T1-weighted hyperintensity of GP was appreciated in only one scan at 14 years of age.

Examination of the SN revealed swelling in 22/27, with T2-weighted hyperintensity in 14/27 cases and T2-weighted hypointensity in 12/27; SN hyperintensity was more common at a younger age (i.e., evident in all MR scans under 2 years of age), whereas hypointensity was more prevalent in older patients (i.e. in all scans over 6 years). On T1-weighted imaging, SN central hyperintensity was seen in 10/27, whereas peripheral hyperintensity was only present in 1/27 scans at 5 years of age. Progressive findings suggestive of SN iron accumulation, such as evolving T2-weighted hypointensity and T1-weighted central hypointensity with or without peripheral hyperintensity, were evident in 5/15 follow up scans. The typically reported 'T1 halo' sign was not seen in our cohort.

SWI sequences were available in 19/27 scans. Features consistent with iron deposition (e.g. hypointensity in Minimum Intensity Projection algorithm images[11]) were seen in 12/19 scans, the earliest noted in a patient (B06) at 3 years of age (range 3 - 14 years, mean age 6.8 years, median 6 years). All cases with features consistent with GP iron deposition (12/19) also showed SN iron deposition. Moreover, iron deposition was not detectable by SWI in early childhood (only evident in 2/12 children under 4 years of age, and in 2/15 scans in this age group overall). Conversely, iron was seen on SWI in 6/7 patients (7/8 scans total) imaged at 5 years or older. When comparing the GP and SN, the SWI hypointensity was not obviously more prominent in either region. Notably, there were no demonstrable features consistent with iron deposition in the dentate nuclei.

Furthermore, cerebral volume reduction was subjectively seen in 23/27 scans; it was mild in 14/27 (mean age 4.7 years) and moderate in 9/27 (mean age 3.6 years) scans. Bi-caudate ratio measurements were often high (97th percentile or higher for age and sex[12] in 22/27

scans), confirming the above subjective findings and indicating subcortical white matter atrophy[13] (**Table 2**). Progression of cerebral volume reduction was seen in one child (B08, age of first, second and third imaging, 3, 6.5 and 7.5 years respectively). CC thinning was evident in all (27/27) patients, this was mainly diffuse but sometimes with body and posterior predominance. Cerebellar atrophy was subjectively seen in 24/27 scans (13/15 patients); it was mild in 15/27 scans, moderate in 9/27 scans, and progressive in one of the 11 children (B08) who had serial imaging. The volume reduction was restricted to the superior vermis and superior aspect of hemispheres in all cases.

Brainstem findings included a small midbrain (less than 1st percentile) in all (27/27) scans; a small pons (10th percentile or smaller) in 13/27; and relatively large medulla (75th percentile or larger) in 19/27 scans, when compared to reference ranges for age and sex[12] (**Table 2**). In all 27 scans, claval measurements were between 4 and 5mm; claval prominence was evident in 6/27 scans.

Optic nerve measurements in pre-chiasmatic segments were lower than the mean expected for age[14] in all children (0-18 months mean 1.76mm, 1.5-3 years mean 1.8mm, >3years mean 2mm; reference mean values 2.92 mm, 3.08 mm, > 3.2 mm, respectively).

Finally, infrequent MRI findings consisted of reduced myelination[15, 16] (Patient B07, age 1.3 and 5.4 years at first and second scan, respectively), large cerebellum (Patient B04) and hippocampal sclerosis (Patient B14) (n=1 child, each). CT was available in 3 children and showed no pallido-nigral calcification (data not shown).

Discussion

BPAN is an X-linked progressive neurodegenerative condition characterized by brain iron accumulation over time; it initially manifests with non-specific clinico-radiological features including absence of iron accumulation in the basal ganglia. Here, we sought to establish an

early neuroradiological signature that could prompt physicians to consider a diagnosis of BPAN. For this purpose, we analyzed MRI findings from a BPAN paediatric cohort; to our knowledge, is the largest single-center paediatric BPAN neuroradiological study to date.

Firstly, we confirmed the existing literature data that radiological features consistent with brain iron accumulation were not commonly detectable in early childhood[1, 5-7]. Features of iron deposition were only evident in 2 children under 4 years of age (2/15 scans performed at this age) but seen on SWI in 6/7 patients (7/8 scans total) imaged at 5 years of age or above. Moreover, typically reported findings of T2-weighted GP/SN hypointensity and T1-weighted SN hyperintensity only evolved in a minority of children (and mostly where there were large intervals between follow up scans). The typically associated hyperintense 'halo' sign was not seen in our cohort.

Conversely, findings present in early disease - and in almost all scans analyzed - included dentate, GP and SN T2-weighted hyperintensities and swelling, CC and optic nerve thinning, as well as cerebral and cerebellar atrophy. Delayed myelination was only rarely evident (1/15 patients); this is consistent with other studies suggesting abnormal myelination only in a minority of patients (28%)[6]. Additionally, other case reports and small case cohort studies (4 patients or fewer) have also reported GP, SN and deep cerebellar nuclei T2 hyperintensity and swelling in BPAN, which can be transient, and possibly related to pyrexia and seizures[5, 17]. In our cohort, these features tended to persist, with reversal of GP swelling in only 1/11 patients with follow up imaging.

Although individually nonspecific, the constellation of these neuroimaging findings in the appropriate clinical background is highly suggestive of BPAN, which should be suspected. However, similar findings have recently been reported in patients with biallelic *WIPI2* mutations[18]. Interestingly, WIPI2 and WDR45 (also known as WIPI4) both belong in the family of WD-repeat proteins interacting with phosphoinositides (WIPI) and have an essential role in

the early stages of autophagy[19]. Hence, it would be interesting to see if similar radiological patterns emerge in other congenital disorders of autophagy in the future. Moreover, the differential diagnosis should also include other infantile epileptic encephalopathies, other NBIAs, and mitochondrial disorders[20, 21].

From a pathophysiological perspective, it is unclear why GP and SN swelling and T2 hyperintensity predominate early on, with iron deposition becoming obvious at a later age. WDR45 has a role in early autophagy, and it has been postulated that dysfunction in the autophagosome-lysosome degradation pathway might lead to chronic inflammatory changes (that might account for the swelling) and gradual iron deposition in susceptible brain areas[7]. Overall, more research is needed to better understand the underlying mechanisms linking autophagy, iron metabolism and neurodegeneration in BPAN.

Other radiological findings, typically associated with other NBIA disorders were also evident in our cohort. Firstly, optic thinning was present in all patients across all scans, and optic nerve measurements were less than the mean expected for age in all cases[14]. Optic nerve thinning has previously been associated with other NBIA disorders, but not specifically with BPAN[1, 22]. Moreover, optic atrophy is only rarely reported in BPAN[9, 23], and visual electrophysiological testing has not been systematically reviewed. It is possible that these optic nerve abnormalities might contribute to the visual impairment frequently reported in BPAN patients in the clinic[1, 3, 9]. Secondly, cerebellar atrophy was a prominent feature in >85% of our patients; similar findings have been reported in other studies[6, 7, 17], though at much lower frequency (e.g. 23% in one study)[6]. Cerebellar atrophy is also a well-defined radiological feature of other NBIA disorders such as *PLA2G6*-associated neurodegeneration (PLAN) and Fatty acid hydroxylase-associated neurodegeneration (FAHN)[22]. Finally, claval prominence was encountered in 4/15 cases (6/27 scans), which has not previously been reported in BPAN and is more typically associated with PLAN[22]. Notably, the claval prominence in our cohort was milder than that seen in PLAN. Overall, the findings of optic nerve thinning, claval hypertrophy

and cerebellar atrophy provide interesting radiological links with other NBIA disorders[1, 22]. More research is warranted to further characterize these links and elucidate the pathophysiological mechanisms linking BPAN with other NBIAs.

In summary, we describe the largest single-center pediatric neuroimaging study in BPAN. We report a distinct early radiological signature, with dentate, GP and SN swelling and T2 hyperintensity, thin corpus callosum, cerebellar atrophy, optic nerve thinning, and small pontine volume. The early disease neuroradiological features described in this study - even in the absence of iron accumulation - should prompt clinicians to include BPAN in the differential diagnosis, especially in appropriate clinical context. Specifically, lack of iron deposition early in the disease course does not negate the validity of a WDR45 pathogenic variant identified through genetic testing.

ID	Sex	Age	Scans	Mutation	Developmental Delay	Epilepsy	ASD	Sleep Issues	Stereotypies	Other
B01	F	13y 2m	2	c.55+5G>C de novo;	+	+	+	+	-	-
B02	F	8y 8m	2	• c.868C>T p.(Gln290*)	+	-	-	-	+	Febrile seizures in childhood, behavioral issues
B03	F	6y 3m	1	c.404del p.(Lys135Serfs*26)	+	-	-	-	+	Febrile seizures in early childhood
B04	M	7y 11m	2	c.752_754del, p.(Ser251del)	+	-	-	-	-	Non-progressive Lower limb spasticity, failure to thrive
B05	F	14y 8m	2	c.131-2A>G; abnormal splicing	+	+	-	-	+	Right upper limb dystonic posturing on gait
B06	F	10y 3m	3	c.236-18A>G; abnormal splicing[10]	+	+	-	-	-	Metopic suture craniosynostosis
B07	M	5y 2m	2	c.883C>T; p.(Gln295*)	+	+	-	-	-	Axial hypotonia, 4-limb mixed spasticity/ dystonia, pre-axial polydactyly
B08	F	10y 7 m	3	c.400C>T p.(Arg134*)	+	+	-	+	+	Previous febrile seizures
B09	F	22 y	1	c.225_226insA p.(Glu76ArgfsTer39)	+	+	-	-	-	Evolving dystonia and parkinsonian features
B11	F	4y 10 m	1	c.723_724dup p.(Tyr242Serfs*47)	+	+	-	+	-	-
B12	F	5y 9m	2	c.167T>C; p.(Met56Thr)	+	+	+	+	+	Increased appetite
B13	F	13y 3m	2	c.344+2T>A, p.(Ile116Argfs*3)	+	+	-	+	-	Hypersalivation, hyper-pronated feet on gait, challenging behavior
B14	F	10y 8m	2	c.977-6_977delinsTCCCAGA, p.(Ala326Asp)	+	+	-	-	-	myopia/strabismus
B15	F	9y 7m	1	•c.233C>A, p.(Ser78*)	+	+	-	+	-	Challenging behavior, insatiable appetite
B18	F	3y 11m	1	c.666del, p.(Asp222Glufs*66)	+	+	-	-	-	Hypersalivation, Increased appetite

Table 1. Cohort Demographics. *An overview of patients is shown. Only paediatric patients (< age of 18 years at the time of first neuroimaging) were included and the majority were female. Abbreviations: Age= Patient current age, ASD= autism spectrum disorder, F= female, ID= identification, M= male, += feature present, -= feature absent*

Patient ID	Age at scan (y)	Midbrain (mm)	Centile	Pons (mm)	Centile	Medulla (mm)	Centile	BC Ratio	Centile
B1	1.9	12	<1	17	25	11	75	0.084	50
	11	12	<1	19	3	13	75	0.069	50
B2	1.2	11	<1	16	25	11	75	0.147	>99
	4	13	<1	19	50	12	75	0.091	90
B3	4	10	<1	18	25	11	25	0.102	99
B4	1	9	<1	16	10	9	3	0.142	>99
	5	9.5	<1	18	3	11	25	0.136	>99
B5	4	10	<1	19	25	13	>99	0.128	>99
	10	12	<1	20	10	13	90	0.101	>99
B6	2.9	8	<1	15	<1	10	25	0.133	>99
	3	9	<1	16	1	11	50	0.107	99
	4	9	<1	18	25	11	50	0.107	>99
B7	1.3	11	<1	17	25	13	>99	0.208	>99
	5.4	10	<1	17	<1	13	90	0.21	>99
B8	3	10	<1	15	<1	12	97	0.099	97
	6.5	10	<1	16	<1	11	50	0.138	>99
	7.5	11	<1	16	<1	11	50	0.142	>99
B9	14	11	<1	19	<1	13	75	0.125	>99
B11	0.8	9	<1	18	75	10	75	0.081	25
B12	1.8	10	<1	19	75	12	>99	0.126	>99
	3	11	<1	20	75	12	97	0.136	>99
B13	1.3	10	<1	17	25	12	>99	0.113	99
	5.3	12	<1	20	25	12	75	0.09	97
B14	1.5	9	<1	18	50	12	>99	0.121	>99
	3	10	<1	19	50	13	>99	0.145	>99
B15	8.3	12	<1	19	3	13	90	0.074	75
B18	1.5	9	<1	16	3	11	90	0.119	>99

Table 2. Midbrain and supratentorial measurements in our cohort. All BPAN patients have small midbrain sizes, as well as pons sizes that are also either small, or relatively small compared to the size of the medulla. Bicaudate ratios are often high, indicating cerebral/ sub-cortical white matter atrophy. Abbreviations: BC= bicaudate, ID= identification, mm= millimeters, y= years
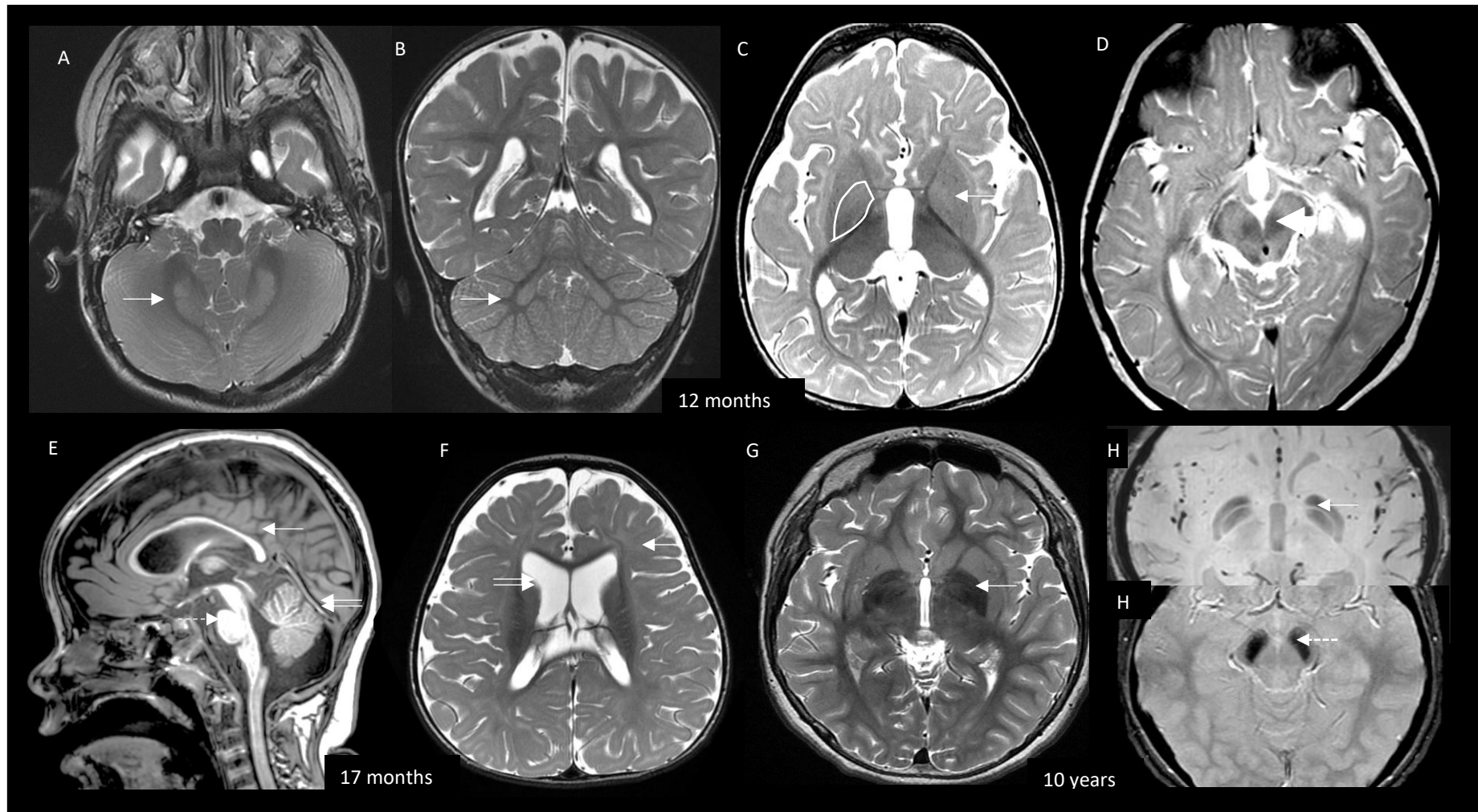
Figure 1. BPAN Early Radiological Signature. At 12 months of life: axial and coronal T2 (A,B) images show bilateral symmetric dentate nucleus hyperintensity and swelling (white arrows). Axial T2 (C) shows bilateral globus pallidus swelling and mild hyperintensity (white arrow). Bilateral substantia nigra swelling and T2 hyperintensity is demonstrated on image D (white arrow). At 17 months: mid sagittal T1 (E) shows diffuse callosal thinning (white arrow), small pons (dotted arrow)

and superior vermian volume loss (double arrow). Axial T2 (F) shows diffuse myelin reduction (white arrow) and prominent lateral ventricles (double arrow). Delayed myelination was infrequently seen in out cohort (1/15 patients). At 10 years: T2 axial image (G) in an older child shows globus pallidus iron deposition which is confirmed on SWI (H). Image H' also shows increased iron deposition in the substantia nigra. The typically reported 'T1 halo sign' was not seen in our paediatric cohort.
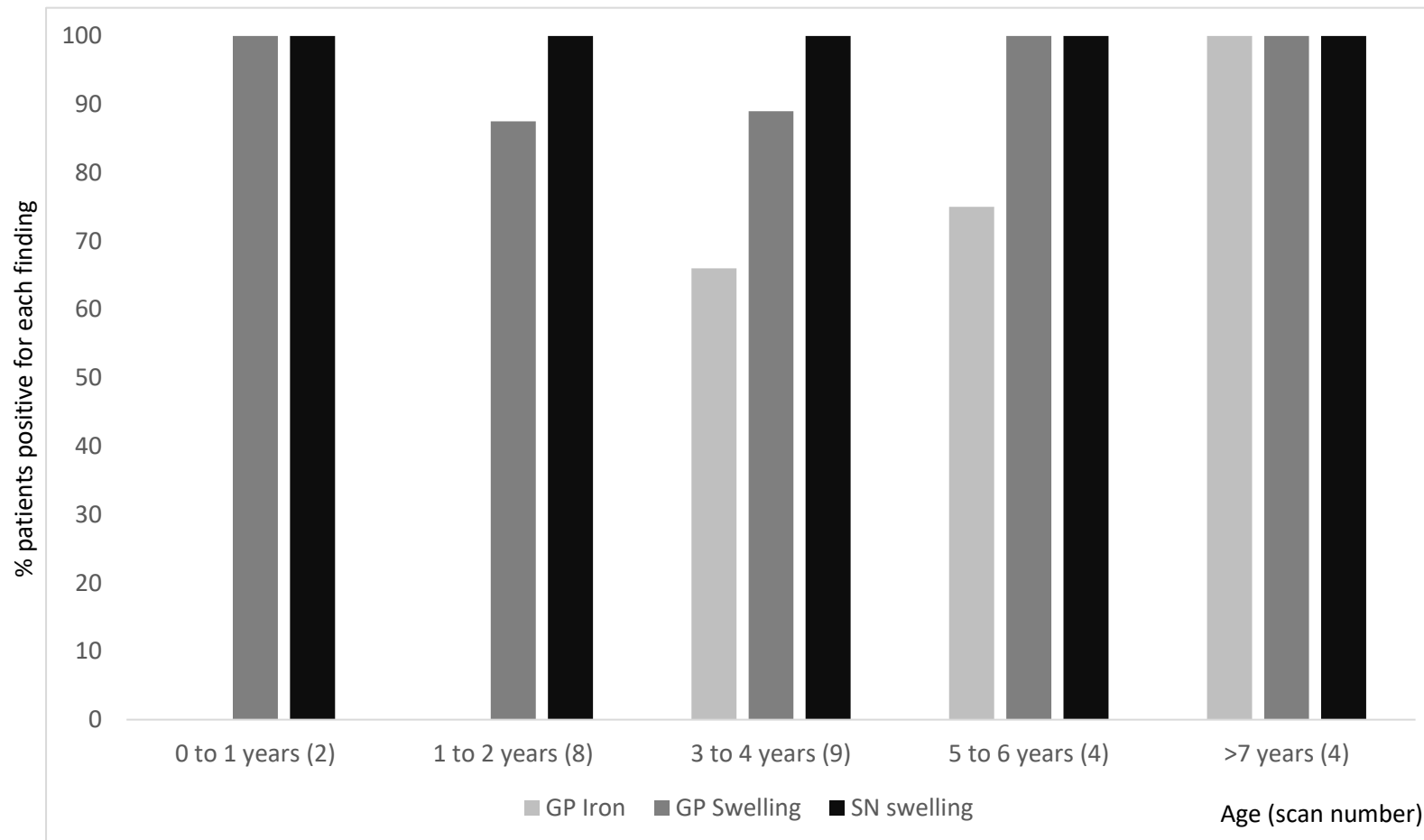

Figure 2. MRI Findings in relation to age. *GP iron deposition is not detectable early on but becomes more prominent after the age of 4 years. Conversely, Globus pallidus and substantia nigra swelling are findings present in young patients and persistent later on. Regarding globus pallidus swelling, this was absent in one patient (B14, two scans at age of 1.5 and 3 years), but otherwise consistently present in all patients and all scans. Abbreviations: GP: globus pallidus, SN: substantia nigra.*

REFERENCES

1.   Wilson JL, Gregory A, Kurian MA, et al. Consensus clinical management guideline for beta-propeller protein-associated neurodegeneration. *Developmental medicine and child neurology* 2021

2.   Saitsu H, Nishimura T, Muramatsu K, et al. De novo mutations in the autophagy gene WDR45 cause static encephalopathy of childhood with neurodegeneration in adulthood. *Nature genetics* 2013;45:445-449, 449e441

3.   Hayflick SJ, Kruer MC, Gregory A, et al. beta-Propeller protein-associated neurodegeneration: a new X-linked dominant disorder with brain iron accumulation. *Brain* 2013;136:1708-1717

4.   Paudel R, Li A, Wiethoff S, et al. Neuropathology of Beta-propeller protein associated neurodegeneration (BPAN): a new tauopathy. *Acta neuropathologica communications* 2015;3:39

5.   Kimura Y, Sato N, Ishiyama A, et al. Serial MRI alterations of pediatric patients with beta-propeller protein associated neurodegeneration (BPAN). *J Neuroradiol* 2021;48:88-93

6.   Adang LA, Pizzino A, Malhotra A, et al. Phenotypic and Imaging Spectrum Associated With WDR45. *Pediatric neurology* 2020;109:56-62

7.   Russo C, Ardissone A, Freri E, et al. Substantia Nigra Swelling and Dentate Nucleus T2 Hyperintensity May Be Early Magnetic Resonance Imaging Signs of β-Propeller Protein-Associated Neurodegeneration. *Mov Disord Clin Pract* 2019;6:51-56

8.   Schulz A, Ajayi T, Specchio N, et al. Study of Intraventricular Cerliponase Alfa for CLN2 Disease. *The New England journal of medicine* 2018;378:1898-1907

9.   Gregory A, Kurian MA, Haack T, et al. Beta-Propeller Protein-Associated Neurodegeneration. In: Adam MP, Ardinger HH, Pagon RA, et al., eds. *GeneReviews((R))*. Seattle (WA): University of Washington, Seattle
University of Washington, Seattle. GeneReviews is a registered trademark of the University of Washington, Seattle. All rights reserved.; 2016

10.   Willoughby J, Duff-Farrier C, Desurkar A, et al. Functional mRNA analysis reveals aberrant splicing caused by novel intronic mutation in WDR45 in NBIA patient. *American journal of medical genetics Part A* 2018;176:1049-1054

11.   Halefoglu AM, Yousem DM. Susceptibility weighted imaging: Clinical applications and future directions. *World J Radiol* 2018;10:30-45

12.   Garbade SF, Boy N, Heringer J, et al. Age-Related Changes and Reference Values of Bicaudate Ratio and Sagittal Brainstem Diameters on MRI. *Neuropediatrics* 2018;49:269-275

13.   Bermel RA, Bakshi R, Tjoa C, et al. Bicaudate ratio as a magnetic resonance imaging marker of brain atrophy in multiple sclerosis. *Archives of neurology* 2002;59:275-280

14.   Maresky HS, Ben Ely A, Bartischovsky T, et al. MRI measurements of the normal pediatric optic nerve pathway. *J Clin Neurosci* 2018;48:209-213

15.   McErlean A, Abdalla K, Donoghue V, et al. The dentate nucleus in children: normal development and patterns of disease. *Pediatr Radiol* 2010;40:326-339

16.   A. James Barkovich CR. Pediatric Neuroimaging, 6th ed. 2018

17.   Ishiyama A, Kimura Y, Iida A, et al. Transient swelling in the globus pallidus and substantia nigra in childhood suggests SENDA/BPAN. *Neurology* 2018;90:974-976

18.   Maroofian R, Gubas A, Kaiyrzhanov R, et al. Homozygous missense WIPI2 variants cause a congenital disorder of autophagy with neurodevelopmental impairments of variable clinical severity and disease course. *Brain Commun* 2021;3:fcab183

19.   Proikas-Cezanne T, Takacs Z, Donnes P, et al. WIPI proteins: essential PtdIns3P effectors at the nascent autophagosome. *Journal of cell science* 2015;128:207-217

20.   Gregory A, Hayflick S. Neurodegeneration with Brain Iron Accumulation Disorders Overview. In: Adam MP, Everman DB, Mirzaa GM, et al., eds. *GeneReviews(®)*. Seattle (WA): University of Washington, Seattle

21.   Saneto RP, Friedman SD, Shaw DW. Neuroimaging of mitochondrial disease. *Mitochondrion* 2008;8:396-413

22.   Hayflick SJ, Kurian MA, Hogarth P. Neurodegeneration with brain iron accumulation. *Handbook of clinical neurology* 2018;147:293-305

23.   Rathore GS, Schaaf CP, Stocco AJ. Novel mutation of the WDR45 gene causing beta-propeller protein-associated neurodegeneration. *Movement disorders : official journal of the Movement Disorder Society* 2014;29:574-575